

Enhancing power conversion efficiency of polycrystalline silicon solar cells through ZnO/SiO₂/Al₂O₃ anti-reflective coatings via spin coating

T.Anu^a, U. Gobikrishnan^b, S. Karthikeyan^{c,*}, S. Chirag^d, S. Vishal^e,
N. Aravindan^f, S. Swathi^g

^aDepartment of Multidisciplinary Engineering, The NorthCap University,
Gurugram

^bDepartment of Mechanical Engineering, Sona College of Technology, Salem

^cDepartment of Mechanical Engineering, Erode Sengunthar Engineering College,
Perundurai, Erode- 638057

^dDepartment of product design, DLC state university of performing and visual
arts, Rohtak

^eDepartment of Mechanical Engineering, Ramdeobaba University, Nagpur -
440013

^fDepartment of Fire Engineering, National Fire Service College, Nagpur

^gDepartment of Physics, Agni College of Technology, Chennai

The investigation aims to enhance the photocurrent generation of p-Si solar cells through the application of anti-reflective coatings (ARC) including ZnO, SiO₂, Al₂O₃, and a combination of ZnO, SiO₂, and Al₂O₃. The spin coating approach was preferred for depositing anti-reflective coating materials as clear thin films on the substrate of the p-Si cells. The absorbance, reflectance, I-V, morphology, and temperature behaviour of the ARCs on p-Si cells were examined to ascertain the impact of the ARCs. Among several coating materials, the blended ZnO+SiO₂+Al₂O₃ on p-Si cells achieved a highest conversion efficiency of 20.71% under controlled setup condition, with an electrical resistance of $5.83 \times 10^{-3} \Omega \text{ cm}$. The examination of the optical characteristics demonstrated a highest absorbance of 92% and a lowest reflection loss of 10%, attained by the ZnO+SiO₂+Al₂O₃ sample within UV band. The ZnO+SiO₂+Al₂O₃ blend exhibited significant enhancement in thermal behaviour, achieving a lowest temperature of 49.9 °C in controlled source settings. Analyses demonstrated that the composite ZnO+SiO₂+Al₂O₃ is a suitable blend with an ideal anti-reflective properties to improve the efficiency of p-Si solar panels.

(Received November 3, 2024; Accepted January 23, 2025)

Keywords: Solar power, Solar cell coating, Optical properties and electrical characteristics

1. Introduction

With the increasing need for sustainable energy solutions, continuous research seeks to improve solar cell performance and decrease costs, establishing them as a crucial element of the global energy framework [1, 2]. By utilizing the photovoltaic principle, solar panels are electronic components that convert solar power into electricity. This process entails the photon absorption by semiconductor materials, resulting in the excitation of electrons and the generation of electrical energy [3]. Antireflection coatings (ARCs) are essential for maximizing the performance of polycrystalline silicon cells by eliminating reflection loss and enhancing photon absorbance. Bare silicon surfaces can reflect more than 30% of incident sunlight, so considerably diminishing the quantity of light available for conversion into power. Anti-reflective coatings (ARCs) are engineered to diminish reflection via optical interference, hence improving the PCE of solar cells.

The core principle of ARCs relies on the destructive interference. The light reflected from the ARC's top surface can be made to be in phase with the light reflection from the solar panel rear

* Corresponding author: karthiksamynathan@gmail.com

<https://doi.org/10.15251/JOR.2025.211.75>

surface by applying a thin coating of dielectric material of a particular thickness. At specific wavelengths, these two waves destructively interfere with one another, canceling each other out and lowering the net reflection to almost zero [4]. It is common practice to adjust the ARC's thickness to $1/4$ of the light's wavelength in the dielectric material for maximum performance. At wavelengths near 600 nm, which is near the sun spectrum's intensity peak, this design minimizes reflection.

Materials such as MoSe_2 , MoS_2 , CaTiO_3 , TiO_2 , SiO_2 , MnFe_2O_4 , Ta_2O_5 , ZnAl_2O_4 , ZnAl_2S_4 , etc. are utilized as ARCs to improve light transmittance by decreasing reflection [5-8]. The standard materials of ARCs consist of silicon dioxide (SiO_2) and silicon nitride (SiN). One of the main reasons why screen-printed solar cells are so popular is because silicon nitride has two uses: reducing reflection and passivating surface imperfections that cause recombination losses [9]. Many investigations have been performed on thin films consisting of transparent conductive oxide (TCO) that are employed across various optoelectronic devices such as solar energy devices, LED's, and display devices [10]. Double-layer antireflective coatings, such as $\text{SiO}_2/\text{TiO}_2$, attained efficiencies of 22.82% and the greatest external quantum efficiency [11]. Triple-layer ARCs with varied refractive indices exhibit improved efficiency through the down-conversion of ultraviolet photons [12]. Reflectance was reduced to 5.71% with three-layer antireflective coatings, in contrast to 34.66% for single-layer coatings [13].

Graded SiN sheets markedly diminished surface reflection, hence improving efficiency in multicrystalline silicon cells [14]. Antireflective coatings were applied to optical devices by diverse physical deposition methods, including molecular beam epitaxy (MBE), electron beam evaporation (E-beam), atomic layer deposition (ALD), spin coating, dip coating and magnetron sputtering [15]. Under optimal conditions, SLARCs can diminish reflectance to approximately 2.5% within a restricted spectral band. The amount of reflection is frequently excessive for numerous applications, constraining the overall efficiency of the solar cells. Conversely, multi-layer anti-reflection coatings (MLARCs) can attain markedly reduced reflectivity over an extensive spectrum of wavelengths [16]. A single-layer ARC significantly reduces reflections over a narrow band of wavelengths. It is necessary to adjust ARCs to satisfy the demands of modern equipment and product improvement.

The fundamental purpose of this scientific investigation is to employ a mixture of ZnO , SiO_2 , and Al_2O_3 as the antireflective coating material for polycrystalline silicon photovoltaic cells by the spin coating procedure. The absorbance, reflectance, I-V, morphology, and temperature behaviour of $\text{ZnO}+\text{SiO}_2+\text{Al}_2\text{O}_3$ nano-layers placed on solar cells are examined comprehensively. The entire schematic representation is provided in fig. 1.

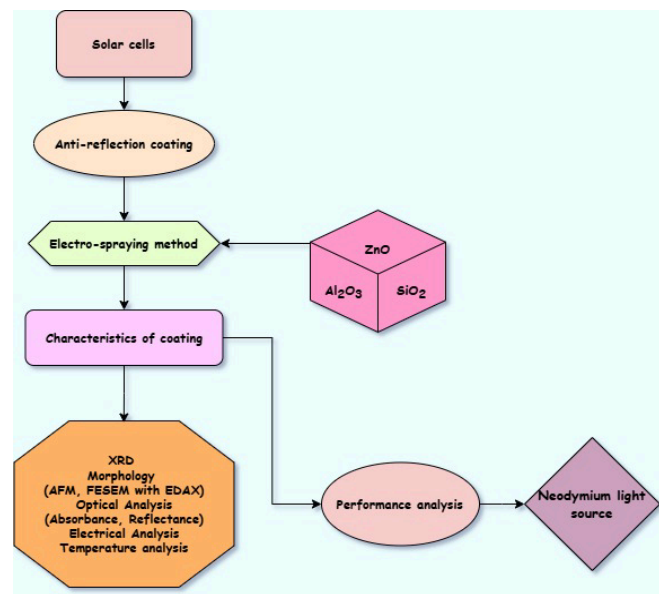


Fig. 1. Diagrammatic flowchart of entire deposition process.

2. Methodologies for experimentation

2.1. Materials

The materials used for ARC deposition process such as ZnO, SiO₂ and Al₂O₃ were bought from Sigma Aldrich. The polycrystalline silicon solar cell measuring 52 mm length and 38 mm breadth were bought from Vikram Solar, India.

2.2. Spin coating of ARC materials on solar cells

The identical quantity of acquired powders was placed into the mortar and pestle apparatus. Subsequently, both combinations were crushed mechanically for approximately three hours. The solvent was formulated by dissolving 0.1 g of ZnO, SiO₂, Al₂O₃, and a mixture of ZnO, SiO₂, and Al₂O₃ powders in 10 ml of ethanol, accompanied by continuous stirring at the ambient temperature for 1 hour. The obtained solvent has been sonicated for 5 minutes and thereafter stirred continuously for 20 minutes at ambient temperature. Before depositing ARCs, the P-si solar cell samples were cleansed with ethanol. The sol solution was applied to solar cell samples by the spin coating process. A uniform speed of 2500 rpm and a duration of 40 seconds were consistently upheld for all coating materials.

2.3. Characterization methods

The X'Pert PRO analyzer was used to conduct X-ray diffraction analyses of the materials, revealing their crystal structure and structural characteristics. The roughness of the ARC deposited cells was investigated utilizing atomic force microscopy (AFM). The surfacemorphology of several ARC samples was measured using a FESEM. An EDX spectrometer was used to examine the coated specimen's chemical constituents. The absorbance and reflections of ARC specimens were validated utilizing UV spectroscopy. The IV properties of ARC cells were assessed using a Keithley 2450 device. Thermal analysis of several ARC cells was conducted using an IR thermo-imaging method.

3. Findings and discussion

The XRD method facilitates the investigation of structural characteristics of bare, ZnO, SiO₂, Al₂O₃, and blended ZnO+SiO₂+ Al₂O₃ coated cells as shown in fig.2. The existence of silicon peaks in all the ARC deposited cells represents the coated cells are made up of crystalline silicon. The acquired XRD peak intensities correspond to the typical JCPDS cards: ZnO (JCPDS No. 43-0002), SiO₂ (JCPDS No. 33-1161) and Al₂O₃ (JCPDS No. 46-1212), therefore confirming the existence of ZnO, SiO₂, and Al₂O₃. The crystal structures of the ZnO, SiO₂, and Al₂O₃ (tetrahedral) nanoparticles were analyzed using XRD imaging.

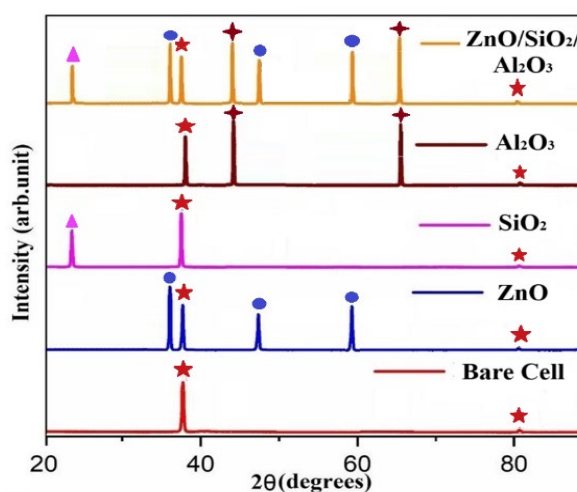


Fig. 2. Crystalline nature of bare and various ARC solar cell samples.

Fig. 3 illustrates the surface topology and roughness of ARC cells as determined by AFM examination. The mean roughness values of ARCs was assessed using tapping method. The tested surface roughness of several materials, including ZnO, SiO₂, Al₂O₃, and a mix of ZnO, SiO₂, and Al₂O₃, was 107 nm, 111 nm, 117 nm and 144 nm, respectively. The physically mixed ZnO+ SiO₂+ Al₂O₃ cells demonstrates highest surface texture value because of combined ARC characteristics on the p-Si cells. This enhances the light capturing ability of the solar cell due to surface irregularities.

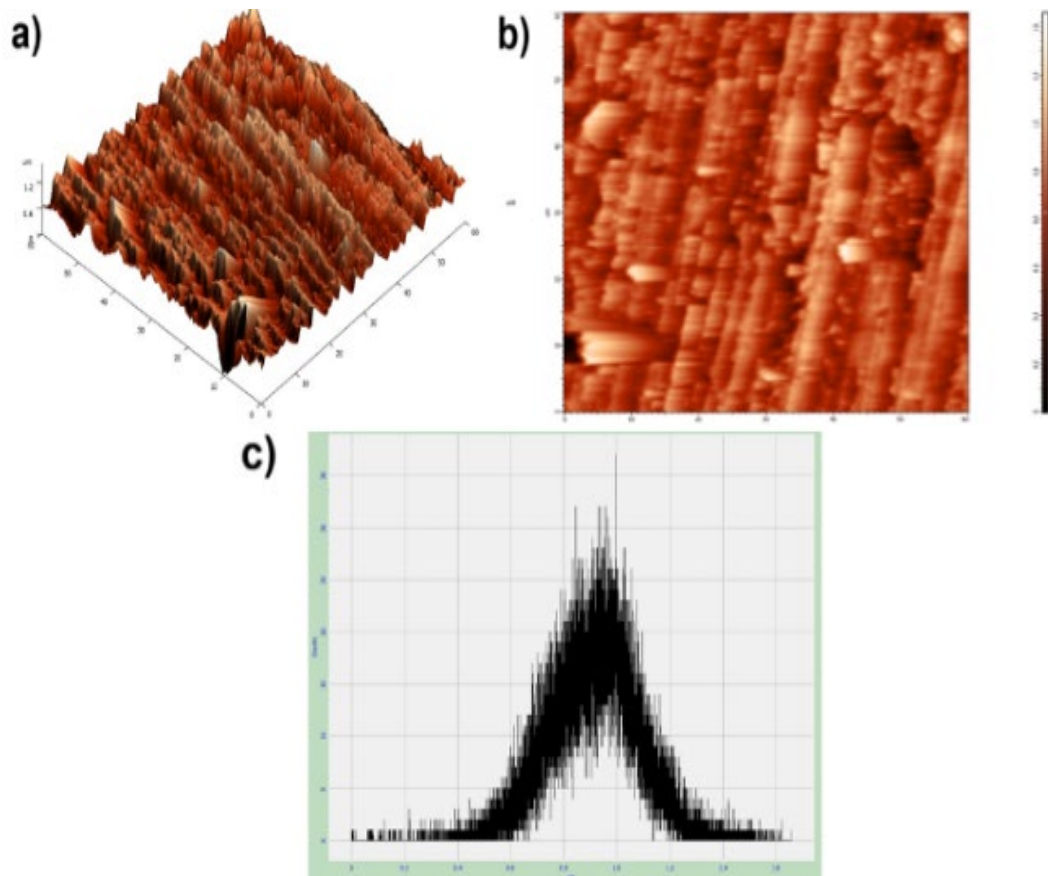


Fig. 3. Surface texture evaluation (3D & 2D) of ZnO+SiO₂+Al₂O₃ coated solar cell sample.

FESEM experimentation is utilized to acquire the ARC microstructure and a cross-section thickness of ZnO+SiO₂+Al₂O₃ coating sample, as seen in fig. 4a and 4b.

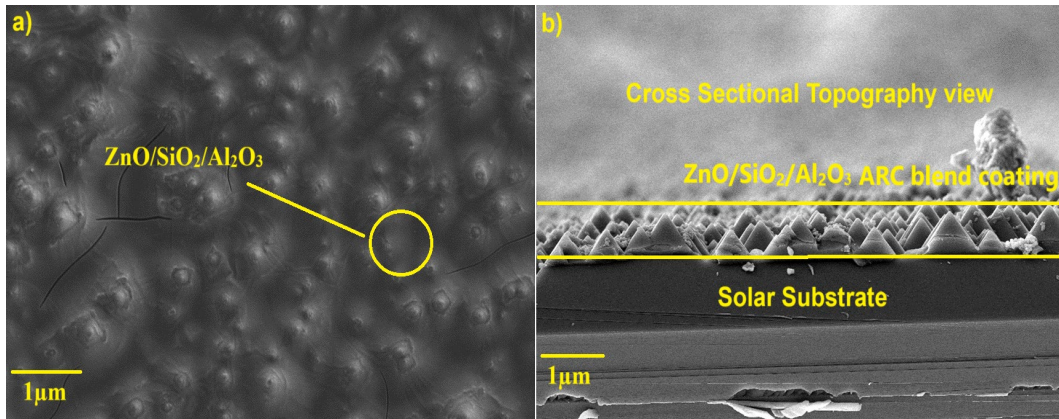


Fig. 4. FESEM – (a) ARC Morphology and (b) cross-sectional thickness of $ZnO+SiO_2+Al_2O_3$ coated solar cell sample.

As seen, there exists uniformity in the deposition of ARC material over the surface of p-Si cells. The width (thickness) of ARCs for ZnO, SiO₂, Al₂O₃ and blended ZnO+SiO₂+Al₂O₃ specimens are 667 nm, 689 nm, 696 nm and 769 nm.

From fig. 5, it is clear that EDAX investigation illustrates the varying elements levels present in ARCs applied Si cells. The detected crests indicate a significant presence of Zn, Si, Al, and O in the ZnO+SiO₂+ Al₂O₃ specimens, as seen in fig. 5. The maximum level of silicon (Si) in fig. 5 may be validated by employing p-Si solar cells for coating.

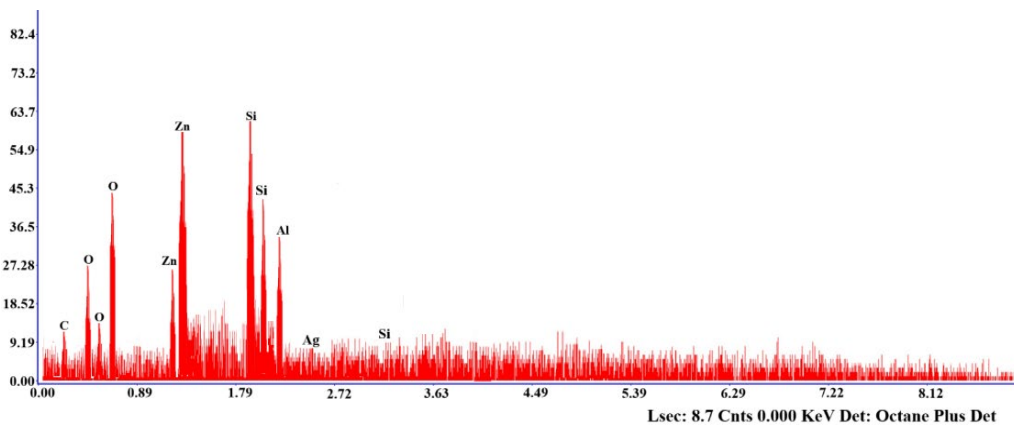


Fig. 5. EDAX compositional analysis of $ZnO+SiO_2+Al_2O_3$ applied p-Si cell.

The absorbance and reflection analysis of bare and ARC applied samples are depicted in fig. 6. The ZnO+SiO₂+ Al₂O₃ coated solar cell exhibited a reduced reflectance of 10% compared to both untreated and other coated solar cells, attributable to the superior passivity provided by the combined layer. The reduced reflectance of the ZnO+SiO₂+ Al₂O₃ coated sample results from the increased surface roughness of the combined layer sample, which leads to minimum diffraction of sunlight that hits at the cell surface [17]. Due to maximum surface texture, incoming light gets stuck in cracks, leads to large interior reflectance, which significantly diminishes reflectance loss [18].

Table 1. Optical properties of bare and ARC applied p-Si cells.

Specimen	Absorbance (%)	Reflection (%)
Bare cell	75	24
ZnO	80	20
SiO ₂	85	15
Al ₂ O ₃	88	12
ZnO+SiO ₂ +Al ₂ O ₃	92	10

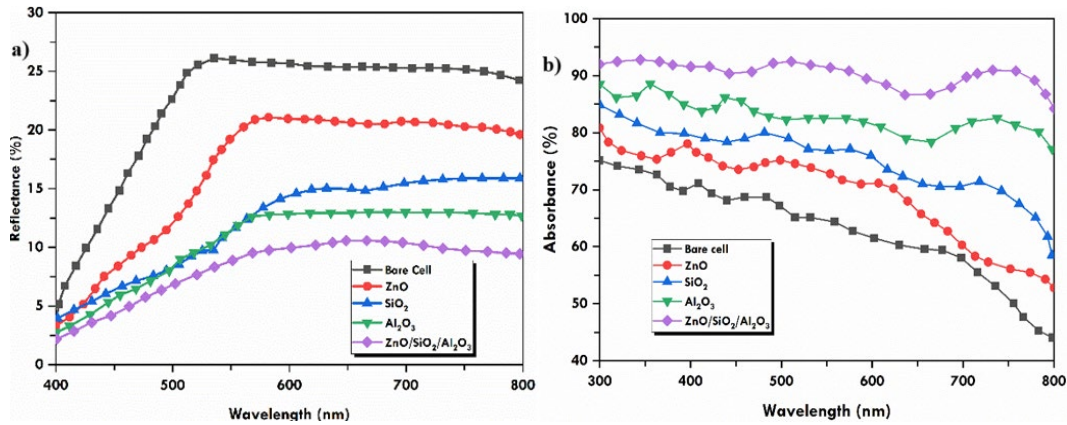


Fig. 6. (a) Reflection and (b) Absorbance of bare and various ARCs applied p-Si cells.

From fig. 6, it is observed that the ZnO+SiO₂+ Al₂O₃ coated specimen has the highest absorbance of 92%. The optical absorbance increases in an ordered sequence: ZnO+SiO₂+ Al₂O₃>Al₂O₃>SiO₂>ZnO, whereas reflectance falls correspondingly, as detailed in Table 1. The values of absorbance indicate that the application of ARCs enhances transmission and absorption of irradiation while minimizing reflection, hence improving the light capture and PCE of p-Si cells. The superior absorbance of the ZnO+SiO₂+ Al₂O₃ applied on Si cells results from the efficient surface interface contact that improves light capture.

Using a four-probe approach, the electrical resistivity, carrier concentration, and hall mobility of solar cell specimens were analyzed as depicted in fig. 7. As observed, ZnO+SiO₂+ Al₂O₃ coated solar cell exhibits low electrical resistance of $5.83 \times 10^{-3} \Omega \text{ cm}$. The bare cell possesses the highest resistivity of $7.42 \times 10^{-3} \Omega \text{ cm}$. The resistance diminishes as light transparency and carrier concentration rise, as illustrated in Table 2. It is noted that the ZnO+SiO₂+ Al₂O₃ blended coating achieves the maximum hall mobility ($15.26 \text{ cm}^2 \text{ V}^{-1} \text{ s}^{-1}$) and carrier concentration ($36.56 \times 10^{20} \text{ cm}^{-3}$). The coating of bigger grain-sized materials with diminished grain boundaries significantly enhances the rate of exciton production and recombination. [16, 19]. The exciton mobilization escalates with the augmentation of photocurrent generation and light intensity.

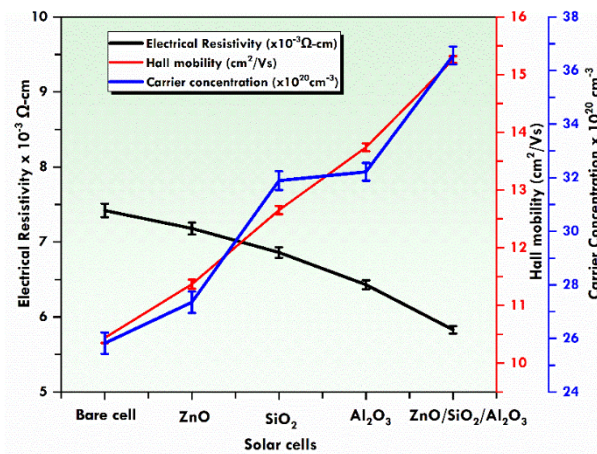


Fig. 7. Electrical features of bare and various ARCs applied p-Si cells.

Table 2. Electrical characteristics of bare and various ARC p-Si cells.

Specimen	Electrical Resistance (Ω cm)	Carrier concentration (cm^{-3})	Hall mobility ($\text{cm}^2 \text{V}^{-1}\text{s}^{-1}$)
Bare cell	7.42×10^{-3}	25.82×10^{20}	10.44
ZnO	7.18×10^{-3}	27.35×10^{20}	11.37
SiO ₂	6.86×10^{-3}	31.89×10^{20}	12.65
Al ₂ O ₃	6.43×10^{-3}	32.22×10^{20}	13.74
ZnO+SiO ₂ +Al ₂ O ₃	5.83×10^{-3}	36.56×10^{20}	15.26

Fig. 8 illustrates the I-V curves of bare, ZnO, SiO₂, Al₂O₃, and a mix of ZnO+SiO₂+ Al₂O₃ coated p-Si cells at regulated environment, irradiated by 1000 W/m² (one sunlight exposure) neodymium light. The manipulation of incoming light was conducted using a pyranometer and an AC regulator. The pyranometer measures the intensity of incoming light, while the AC regulator modulates the light. Correspondingly, the PCE of the solar cell specimens was assessed using the I-V pattern and detailed in Table 3.

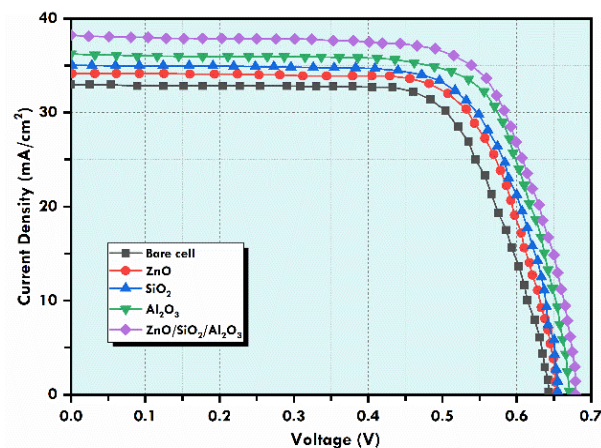


Fig. 8. I-V trajectory of bare and various ARCs applied p-Si cells.

The output measurements of voltage and current were measured and transformed into an I-V profile, from which the productivity may be determined. The bare cell achieves a power conversion efficiency (PCE) of 15.14% with parameters: $J_{sc} = 32.91 \text{ mA/cm}^2$, $V_{oc} = 0.63 \text{ V}$, $FF = 73$). The ZnO+SiO₂+ Al₂O₃ coated silicon solar exhibits enhanced output photocurrent production (PCE = 20.71% $J_{sc} = 38.23 \text{ mA/cm}^2$, $V_{oc} = 0.678 \text{ V}$, and $FF = 80\%$). An increase in J_{sc} and V_{oc} results in a rise in PCE from 15.14% to 20.71% in closed system conditions. The enhancement of fill factor results in a corresponding rise in productivity [20].

Table 3. I-V properties of bare and ARCs applied p-Si cells.

Sample	Voltage $V_{oc}(V)$	Current Density $J_{sc}(\text{mA/cm}^2)$	FF (%)	PCE (%)
Bare cell	0.63	32.91	73	15.14
ZnO	0.652	33.98	74	16.33
SiO ₂	0.655	34.71	76	17.26
Al ₂ O ₃	0.671	36.22	79	19.11
ZnO/SiO ₂ /Al ₂ O ₃	0.678	38.23	80	20.71

Fig. 9 illustrates the thermal examination of (a) ZnO, (b) SiO₂, (c) Al₂O₃, and (d) ZnO+SiO₂+ Al₂O₃ within a closed system condition to measure the surface temperature. The performance of solar cells diminishes as temperature rises. The IR imaging approach is employed to ascertain the operating temperature of various coated solar cells. From the findings, ZnO+SiO₂+ Al₂O₃ exhibits lowest temperature of 49.9 °C than ZnO (57.3 °C), SiO₂ (55.5 °C) and Al₂O₃ (52.3 °C) coated solar cells. The enhanced light scattering elevates the heat flow of solar cells, therefore diminishing the transparency of the anti-reflective coating. Consequently, a lower surface heat significantly improves the productivity of p-Si cells[21]. Thus, it is evident that the ZnO+SiO₂+ Al₂O₃ layer functioned as an exceptional anti-reflective coating material for enhancing the power conversion efficiency.

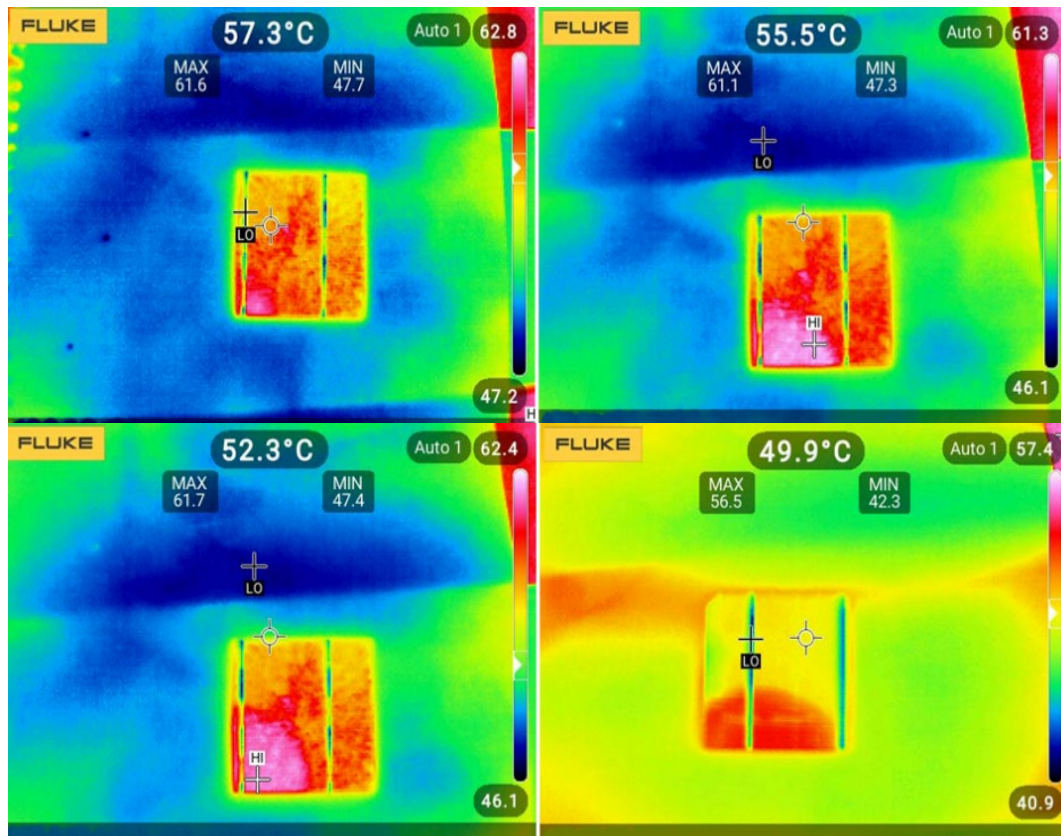


Fig. 9. Surface temperature evaluation of (a) ZnO, (b) SiO₂, (c) Al₂O₃, and (d) ZnO+SiO₂+Al₂O₃ coated solar cells.

4. Conclusion

The blended material of ZnO, SiO₂, and Al₂O₃ was applied to the solar cell surface using the spin coating process. The XRD analysis revealed peak intensities that align with standard JCPDS patterns for ZnO (JCPDS No. 43-0002), SiO₂ (JCPDS No. 33-1161), and Al₂O₃ (JCPDS No. 46-1212), thereby confirming the presence of ZnO, SiO₂, and Al₂O₃ in the sample. The surface roughness of several materials, including ZnO, SiO₂, Al₂O₃, and a mix of ZnO, SiO₂, and Al₂O₃, was 107 nm, 111 nm, 117 nm and 144 nm, respectively. The FE-SEM evaluation reveals the cross-sectional thickness of 667 nm, 689 nm, 696 nm and 769 nm. for the ZnO, SiO₂, Al₂O₃, and a mix of ZnO+SiO₂+ Al₂O₃ coated cells, respectively.

The ZnO+SiO₂+ Al₂O₃ coated solar cell demonstrates an ideal absorbance of 92% and the lowest reflectance of 10% in comparison to bare cells and various ARCs applied on p-Si cells. The p-Si cells with a ZnO+SiO₂+ Al₂O₃ anti-reflective coating exhibited superior PCE, achieving 20.71% under closed conditions. The significant enhancement in the performance of ZnO+SiO₂+ Al₂O₃ applied on p-Si cells may be linked to the reorientation of the morphological behaviour, absorbance, reflectance, I-V, and thermal behaviour of ZnO+SiO₂+ Al₂O₃ applied on p-Si cell substrate.

References

- [1] S. Agarwal, V. Sharma, A. K. Maurya, P. Sen, A. Mishra, AIJR Proceedings (2023).
- [2] G. V. Kaliyannan, R. Rathanasamy, R. Gunasekaran, M. S. Anbupalani, M. Chinnasamy, S. K. Palaniappan, Defect Engineering of Carbon Nanostructures (2022).
- [3] R. Gunasekaran, G. Velu Kaliyannan, U. Gandhi, S. Sivaraj, Journal of Materials Science:

- Materials in Electronics 35(10), (2024); <https://doi.org/10.1007/s10854-024-12417-7>
- [4] T. Markvart, L. Castañer, Practical handbook of photovoltaics: fundamentals and applications. 2003: Elsevier.
- [5] S. Prashanth, R. Rajasekar, V. Gobinath, G. Raja, K. Subha, K. Manjunath, Chalcogenide Letters 18(4), (2021).
- [6] V. Gobinath, R. Rajasekar, C. Moganapriya, A. M. Sri, G. Raja, P. S. Kumar, S. Jaganathan, Chalcogenide Letters 18(7), (2021).
- [7] G. V. Kaliyannan, U. Gandhi, R. Rathanasamy, M. Subramanian, S. Kandasamy, R. Gunasekaran, S. K. Palaniappan, Silicon 15(15), (2023); <https://doi.org/10.1007/s12633-023-02515-2>
- [8] F. H. Alkallas, E. A. Mwafy, G. V. Kaliyannan, R. Gunasekaran, R. Rathanasamy, A. B. G. Trabelsi, W. B. Elsharkawy, A. M. Mostafa, S. K. Palaniappan, Ceramics International 2024).
- [9] H. J. El-Khozondar, R. J. El-Khozondar, R. Al Afif, C. Pfeifer, International Journal of Thermofluids 11(2021); <https://doi.org/10.1016/j.ijft.2021.100103>
- [10] N. Singh, M. Taunk, Transparent metal oxides in OLED devices, in Metal Oxides for Next-generation Optoelectronic Photonic and Photovoltaic Applications. 2024, Elsevier. p. 77-106; <https://doi.org/10.1016/B978-0-323-99143-8.00006-7>
- [11] N. I. I. M. Jamaluddin, M. Z. M. Yusoff, M. F. Malek, Modern Physics Letters B 38(23), (2024); <https://doi.org/10.1142/S0217984924502014>
- [12] J. Zhang, T. Chen, Y. Liu, J. It Wong, Journal of Applied Physics 114(5), (2013); <https://doi.org/10.1063/1.4817821>
- [13] M. S. Sarker, M. F. Khatun, S. R. Al Ahmed, J. Hossain, International Conference on Computer, Communication, Chemical, Materials and Electronic Engineering (IC4ME2). 2019. IEEE; <https://doi.org/10.1109/IC4ME247184.2019.9036677>
- [14] V. Sharma, A. Verma, D. Verma, V. K. Jain, D. Singh, Recent Trends in Materials and Devices: Proceedings ICRTMD 2015. 2017. Springer; https://doi.org/10.1007/978-3-319-29096-6_38
- [15] N. Almakayeel, G. V. Kaliyannan, R. Gunasekaran, Ceramics International 2024).
- [16] E. A. Mwafy, G. V. Kaliyannan, A. Darwish, M. M. Motawea, R. Gunasekaran, R. Rathanasamy, Z. El-Tayeb, W. B. Elsharkawy, A. M. Mostafa, S. K. Palaniappan, Surfaces and Interfaces (2024).
- [17] J. Li, Y. Lu, P. Lan, X. Zhang, W. Xu, R. Tan, W. Song, K.-L. Choy, Solar Energy 89(2013).
- [18] W. Wang, L. Qi, Advanced Functional Materials 29(25), (2019); <https://doi.org/10.1002/adfm.201807275>
- [19] N. Almakayeel, G. V. Kaliyannan, R. Gunasekaran, R. Rathanasamy, Journal of Materials Research and Technology 2024).
- [20] F. H. Alkallas, S. M. Alghamdi, G. V. Kaliyannan, R. Gunasekaran, R. Rathanasamy, A. B. G. Trabelsi, W. Elsharkawy, A. M. Mostafa, S. K. Palaniappan, Ceramics International 50(9), (2024); <https://doi.org/10.1016/j.ceramint.2024.01.402>
- [21] A. Alshammari, E. Almatrafi, M. Rady, Solar Energy 273(2024); <https://doi.org/10.1016/j.solener.2024.112545>